ELSEVIER

Thermochimica Acta 355 (2000) 239–253

thermochimica acta

www.elsevier.com/locate/tca

Kinetic analysis of crystallization processes in amorphous materials

Jiří Málek*

Joint Laboratory of Solid State Chemistry, Academy of Sciences of the Czech Republic and University of Pardubice, 532 10 Pardubice, Czech Republic

Received 10 June 1999; received in revised form 13 September 1999; accepted 26 September 1999

Abstract

Thermal analysis methods are widely used to study crystallization kinetics in amorphous solids. The experimental data is frequently interpreted in terms of the Johnson–Mehl–Avrami (JMA) nucleation-growth model. This paper discusses the limits of such an approach. A simple and convenient method is proposed to verify the applicability of the JMA model as well as the basic assumptions of kinetic analysis. It is shown that the two parameter autocatalytic model includes the JMA model and that is a plausible description of the crystallization kinetics. The main advantage of this model is its flexibility in describing quantitatively the kinetics of complex crystallization processes. The experimental data for crystallization of a chalcogenide glass and zirconia gel analyzed in this paper clearly demonstrate the rather complex nature of these processes. As a consequence, it is very difficult to explore the real mechanism of the crystallization unless some complementary studies are made.

Keywords: Kinetics; Crystallization; Nucleation-growth model; Autocatalytic model; Zirconia; Chalcogenide glass

1. Introduction

Thermal analysis (TA) methods such as DTA or DSC are quite popular for kinetic analysis of crystallization processes in amorphous solids. The crystallization kinetics based on these data is usually interpreted in terms of the standard nucleation-growth model formulated by Avrami [1–3]. This model describes the time dependence of the fractional crystallization α, usually written in the following form:

$$\alpha = 1 - \exp\left[-(Kt)^m\right] \tag{1}$$

where K and m are constants with respect to time, t. The kinetic exponent m depends on the crystal growth morphology [4]. The rate equation can be obtained from Eq. (1) by differentiation with respect to time:

$$\left(\frac{d\alpha}{dt}\right) = Km(1-\alpha)[-\ln(1-\alpha)]^{1-1/m} \tag{2}$$

Eq. (2) is usually referred to as the JMA equation, and it is frequently used for the formal description of TA crystallization data. It should be emphasized, however, that validity of the JMA equation is based on the following assumptions [5–7]:

- Isothermal crystallization conditions,
- Homogeneous nucleation or heterogeneous nucleation at randomly dispersed second-phase particles,
- Growth rate of new phase is controlled by temperature and is independent of time and
- Low anisotropy of growing crystals.

* Fax: +420-40-603-6011.
E-mail address: jiri.malek@upce.cz (J. Málek)

0040-6031/00/$ – see front matter
PII: S0040-6031(00)00449-4

Henderson [5,6] has shown that the validity of the JMA equation can be extended in non-isothermal conditions if the entire nucleation process takes place during the early stages of the transformation, and it becomes negligible afterward. The crystallization rate is defined only by temperature and does not depend on the previous thermal history. Fundamental kinetic equations for non-isothermal crystal growth from preexisting nuclei have been developed by Ozawa [8] and a simple method of kinetic analysis of TA data for these processes has been proposed.

It is clear that all the above mentioned assumptions should be carefully considered before the JMA equation is used for the description of isothermal or non-isothermal TA data and any conclusions concerning the growth morphology are made. Although the limits of applicability of the JMA equation are well known, in practice it is not so easy to verify whether they are fulfilled or not. Thus, in view of the key role of the JMA model in crystallization research, it is important to address this problem. The structure of the paper is as follows. First, we summarize several additional assumptions inherently included in the kinetic analysis of TA data. Second, we propose a consistent method to test all these assumptions as well as the applicability conditions of the JMA model for both isothermal and non-isothermal TA data. Finally, this method is demonstrated using experimental data for crystallization of a chalcogenide glass and zirconia gel.

2. Theory

2.1. Basic assumptions in kinetic analysis

In spite of the importance of the applicability test of the JMA model mentioned above, it is also essential to verify three basic assumptions inherent in any kinetic treatment of isothermal and non-isothermal TA data [9]. These assumptions are formulated below:

1. The rate of the kinetic process $d\alpha/dt$ is proportional to the measured specific heat flow ϕ, normalized per sample mass (W/g):

$$\frac{d\alpha}{dt} = \frac{\phi}{\Delta H_c} \tag{3}$$

where ΔH_c corresponds to the total enthalpy change associated with the crystallization process. The fractional conversion α can be easily obtained by partial integration of isothermal or non-isothermal TA curve.

2. The rate of the kinetic process can be expressed as a product of temperature dependent rate constant $K(T)$ and α dependent kinetic model function $f(\alpha)$:

$$\left(\frac{d\alpha}{dt}\right) = K(T)f(\alpha) \tag{4}$$

3. The rate constant in Eq. (4) follows Arrhenius form:

$$K(T) = A\exp\left(\frac{-E_a}{RT}\right) \tag{5}$$

where the pre-exponential factor A and activation energy E_a are kinetic parameters that should not depend on the temperature T and the fractional conversion α. This assumption is not necessary, e.g. in the case of non-parametric kinetic method described by Serra et al. [10,11].

Taking into account these assumptions, the kinetic equation for the JMA model can be written as

$$\phi = \Delta H_c A\exp\left(\frac{-E_a}{RT}\right)f(\alpha) \tag{6}$$

where the function $f(\alpha)$ is an algebraic expression of the JMA model

$$f(\alpha) = m(1-\alpha)[-\ln(1-\alpha)]^{1-1/m} \tag{7}$$

The $f(\alpha)$ function should be invariable with respect to procedural parameters such as sample mass and heating rate (non-isothermal conditions) or temperature (isothermal conditions).

Fig. 1 shows isothermal and non-isothermal DSC curves calculated by using Eqs. (6) and (7) for the kinetic exponent m=2. The fractional conversion is obtained by integrating Eq. (3) in isothermal conditions:

$$\alpha = \frac{1}{\Delta H_c}\int_0^t \phi\, dt \tag{8}$$

and in non-isothermal conditions

$$\alpha = \frac{1}{\Delta H_c \beta}\int_{T_0}^{T} \phi\, dT \tag{9}$$

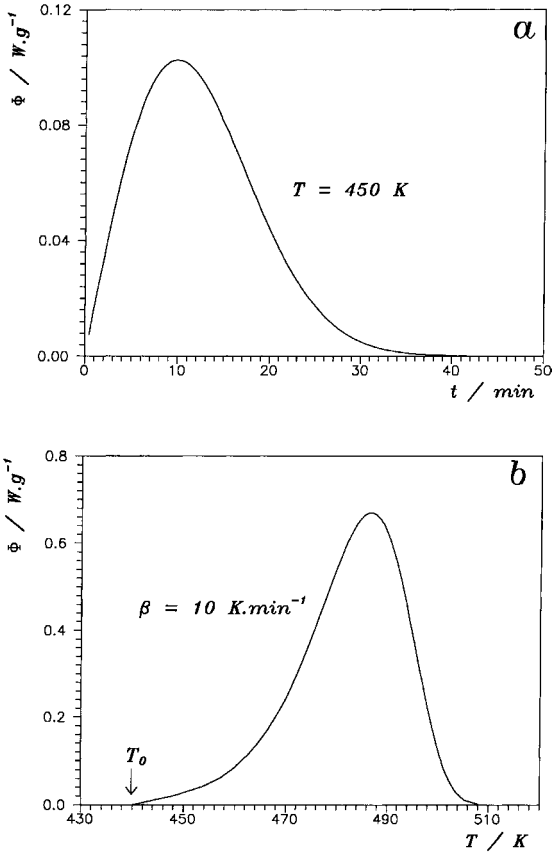

Fig. 1. (a) Isothermal DSC curve calculated for the JMA model (m=2, E_a=100 kJ/mol, ln(A/s)=50); (b) Non-isothermal DSC curve calculated for the same set of kinetic parameters.

where β is the heating rate and T_0 corresponds to the beginning of the baseline approximation (i.e. $\phi(T_0)$=0). The crystallization enthalpy ΔH_c corresponds to the total peak area.

The validity of the assumptions (1)–(3) is not given a priori, and it should be thoroughly verified before any attempt at kinetic analysis of the isothermal or non-isothermal data is made. Thus, it seems to be necessary to develop a simple and reliable testing method. This task will be carried out in the following section.

2.2. Tests of the basic assumptions

The shape and symmetry of the DSC curve that corresponds to the same kinetic model may be quite different in isothermal and non-isothermal conditions (see Fig. 1). Moreover, any direct comparison of the DSC crystallization curves $\phi(T)$ and $\phi(t)$ is complicated by the fact that they strongly depend on the heating rate and temperature, respectively. Nevertheless, the kinetic model $f(\alpha)$ should be invariant with respect to these procedural variables. Similar behavior is expected also for the function defined as $f(\alpha)\int_0^\alpha d\alpha/f(\alpha)$ (see Appendix A). It can be shown [12,13] that these two functions are proportional to the $y(\alpha)$ and $z(\alpha)$ functions that can easily be obtained by a simple transformation of DSC data (see Appendix A). In isothermal conditions these functions are defined as

$$y(\alpha) = \phi \tag{10a}$$

$$z(\alpha) = \phi t \tag{10b}$$

In non-isothermal conditions these functions are defined as follows [12,14]:

$$y(\alpha) = \phi \exp\left(\frac{-E_a}{RT}\right) \tag{11a}$$

$$z(\alpha) = \phi T^2 \tag{11b}$$

For practical reasons the $y(\alpha)$ and $z(\alpha)$ functions are normalized within the (0 1) range. These functions can be written in a more general form using the generalized time concept introduced by Ozawa [8,15] (see Appendix A).

It is evident that the assumption (3) is not necessary for analysis of isothermal experiments, and both the $y(\alpha)$ and $z(\alpha)$ functions directly follow from the experimental data. However, this assumption is vital for analysis of non-isothermal data and the value of apparent activation energy E_a is needed to calculate the $y(\alpha)$ function. The value of E_a can be determined by an isoconversional method without assuming the kinetic model function [16,17]. From the logarithmic form of Eq. (6) it follows that E_a is obtained from the slope of the ln ϕ vs.1/T plot for a constant α:

$$\left[\frac{d\ln\phi}{d(1/T)}\right]_\alpha = -\frac{E_a}{R} \tag{12}$$

This method can be applied to both isothermal and non-isothermal DSC data. The E_a should be practically independent of the fractional conversion in the $0.3 \le \alpha \le 0.7$ range (i.e. within ca. 10%). Some changes may be expected for lower and higher values of α — particularly for fast processes — because of higher errors in the baseline interpolation for peak tails.

The validity of the assumptions (1) and (2) can easily be verified by checking the invariance of the $y(\alpha)$ and $z(\alpha)$ plots with respect to procedural variables such as heating rate (non-isothermal conditions) and temperature (isothermal conditions). These functions should also be identical for both isothermal and non-isothermal DSC data provided that the kinetic model $f(\alpha)$ does not change. In case that there are considerable differences or pronounced influence of the procedural parameters affecting the shape of the $y(\alpha)$ and $z(\alpha)$ functions then, some of these assumptions are probably not fulfilled. Such behavior can be caused by many factors. One possibility is that the baseline has not been drawn correctly due to substantial change of sample heat capacity during the measurement. Another possible explanation is that the measured data corresponds to a complicated process (parallel or consecutive processes, branching, etc.) due to a more complex reaction scheme than expressed by Eq. (6). Thermal inertia effects caused by lower thermal contact between the sample and temperature sensor or low thermal conductivity of amorphous material can also play an important role.

2.3. Tests of the applicability of the JMA model

Probably the most popular testing method for isothermal data is an inspection of the linearity of the Avrami plot; i.e. the dependence of $\ln[-\ln(1-\alpha)]$ as a function of logarithm of time. From logarithmic form of Eqs. (A.5) and (A.10), it follows that the kinetic exponent m is obtained from the slope of this plot:

$$\frac{\mathrm{d}\ln[-\ln(1-\alpha)]}{\mathrm{d}\ln t} = m \tag{13}$$

A similar testing method has also been developed for non-isothermal TA data [9]. From logarithmic form of Eqs. (A.10) and (A.11), it follows that a plot of $\ln[-\ln(1-\alpha)]$ as a function of reciprocal temperature $1/T$ should be linear, provided that the term $\ln[AT\pi(x)/\beta]$ is a constant (see Appendix A). The slope of this plot is expressed as

$$\frac{\mathrm{d}\ln[-\ln(1-\alpha)]}{\mathrm{d}(1/T)} \cong -\frac{mE_\mathrm{a}}{R} \tag{14}$$

The value of the kinetic exponent can then be calculated if the E_a is known. Nevertheless, it is well known that a double logarithmic function, in general, is not very sensitive to subtle changes to its argument. Therefore, one can expect that the plots of $\ln[-\ln(1-\alpha)]$ versus $\ln t$ or $1/T$ may be linear even in the case that the JMA model is not fulfilled [14].

A more reliable test is based on the properties of the $y(\alpha)$ and $z(\alpha)$ functions. These functions exhibit maxima at α_M and α_P^∞, respectively. These maxima are defined by Eqs. (A.3) and (A.9). The maximum of the $y(\alpha)$ function for the JMA model depends on the value of the kinetic exponent:

$$\alpha_\mathrm{M} = 0 \ \text{ for } \ m \leq 1$$
$$\alpha_\mathrm{M} = 1 - \exp\left(m^{-1} - 1\right) \ \text{ for } \ m > 1 \tag{15}$$

The value of α_M is always lower than the maximum of the $z(\alpha)$ function α_P^∞ (see Appendix A). The latter is a constant for the JMA model

$$\alpha_\mathrm{P}^\infty = 0.632 \tag{16}$$

This value is a characteristic 'fingerprint' of the JMA model; and, according to our experience, it can be used as a simple test of the applicability of this model [14]. The value of the kinetic exponent can then be estimated from the position of the maximum of the $y(\alpha)$ function. This is illustrated in Fig. 2 where the DSC data from Fig. 1 transformed by using Eqs. (10) and (11) are shown. The maximum of the $z(\alpha)$ function is located at $\alpha_\mathrm{P}^\infty \cong 0.632$ and, therefore, the curves in Fig. 1 evidently correspond to the JMA model. This is confirmed also by the shape of the $y(\alpha)$ function [12,13] which exhibits a maximum at $\alpha_\mathrm{M} \cong 0.393$. This value corresponds to the kinetic exponent $m=2$, as follows from Eq. (15). It should be pointed out, however, that the typical error limit of α_M and α_P^∞, determined from typical TA data, is ca. ± 0.02. Therefore, the validity of the kinetic model should always be considered within these limits of experimental uncertainty.

An interesting testing method has been proposed by Ozawa [18]. It is based on the plot of $\log[-\ln(1-\alpha)]$ as a function of $\log\beta$ at a given temperature. The slope of such plot should be equal to the kinetic exponent. If the secondary crystallization is negligible then these plots can be superimposed by longitudinal shifts and the master curve is obtained. In contrast, if there is appreciable secondary nucleation, the superposition cannot be made and thus such process can easily be detected [18].

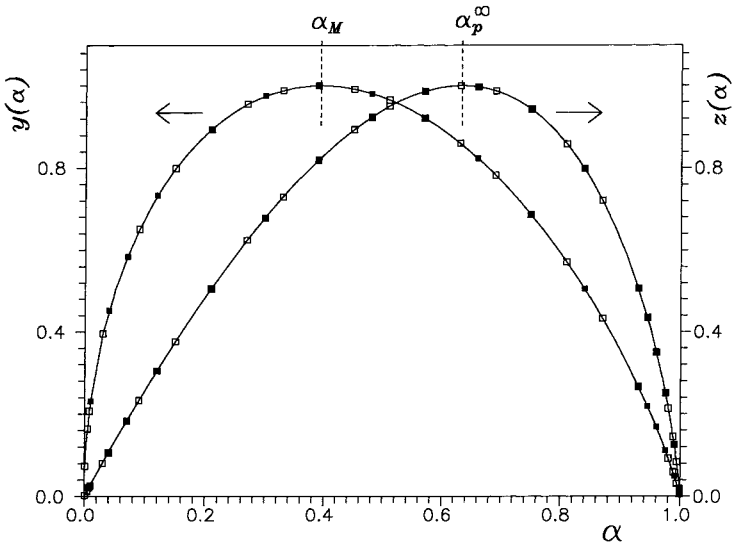

Fig. 2. Normalized $y(\alpha)$ and $z(\alpha)$ function obtained by transformation of DSC data from Fig. 1 by using Eq. (10) for isothermal data (□) and Eq. (11) for non-isothermal data (■). The broken lines show the theoretical α_M value for $m=2$ and the typical α_P^∞ value for the JMA model.

3. Experimental

DSC experiments presented in this paper were performed by using a Perkin–Elmer DSC-7 instrument on samples of ca. 10 mg encapsulated in standard aluminum sample pans in an atmosphere of dry nitrogen. The instrument was calibrated with In, Pb and Zn standards. Non-isothermal DSC curves were obtained with selected heating rates 2–20 K/min in the range 30–600°C. Isothermal DSC experiments were initiated by raising the temperature of the DSC cell from room temperature to the selected temperature, T_i, at 200 K/min. The temperature of the cell was then maintained constant at T_i, and the exothermic heat flow ϕ out of the sample was measured as a function of time.

The $(GeS_2)_{0.3}(Sb_2S_3)_{0.7}$ glass was prepared by synthesis from pure elements (5 N purity) in an evacuated silica ampoule by melting and homogenization at 950°C for a period of 12 h. Amorphous zirconia gel (hydrous ZrO_2) was prepared by precipitation from $ZrOCl_28{\cdot}H_2O$ (analytically pure reagent, Kanto, Japan) 0.1 M solution using an excess amount of 1 M NH_4OH added slowly to a stirred aqueous solution. The precipitated gel was washed five times in distilled water for removal of chloride ions, filtered and dried in a vacuum at room temperature for 3 days. The amorphous nature and purity of prepared materials were checked by X-ray diffraction and energy dispersive microanalysis.

4. Results and discussion

4.1. Crystallization kinetics of $(GeS_2)_{0.3}$ $(Sb_2S_3)_{0.7}$ glass

The crystallization kinetics of chalcogenide glass of $(GeS_2)_{0.3}(Sb_2S_3)_{0.7}$ composition has been described previously [19–23]. Ryšavá et al. [20,21] have found that the crystallization of a bulk sample can be interpreted within the JMA model and reported the kinetic exponent $m=2$. On the other hand, Málek et al. [22,23] have shown that the crystallization of a powder sample cannot be described by this model. These conclusions seem to be confirmed in the present study. Fig. 3 shows isothermal crystallization data for a powder sample and non-isothermal crystallization data for a bulk sample of $(GeS_2)_{0.3}$ $(Sb_2S_3)_{0.7}$ glass. The enthalpy change associated with the crystallization process is $-\Delta H_c^{bulk}=56\pm1$ J/g for the bulk sample, and $-\Delta H_c^{powder}=50\pm2$ J/g for the powder sample. The difference of 6 J/g corresponds approximately to the temperature difference of ca. 25 K between isothermal

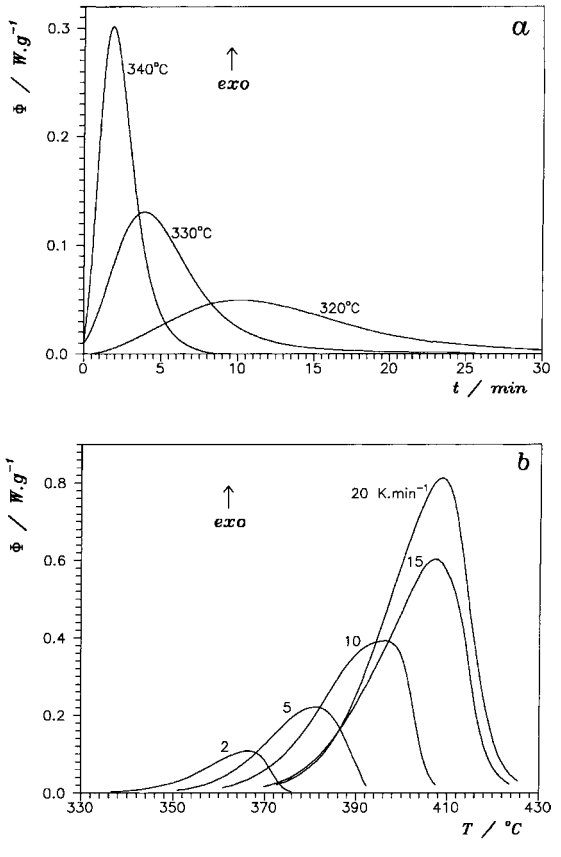

Fig. 3. DSC data for the crystallization of the $(GeS_2)_{0.3}$ $(Sb_2S_3)_{0.7}$ glass: (a) isothermal data for fine powder sample; (b) non-isothermal data for the bulk sample.

and non-isothermal experiments taking into account the heat capacity change between glass and undercooled liquid in the glass transition range ($\Delta C_p \cong 0.24$ J/gK).

Fig. 4 shows the activation energy E_a as a function of fractional conversion calculated by isoconversional method from the slope of the ln ϕ vs. $1/T$ plots for DSC data shown in Fig. 3. The activation energy for the bulk sample is practically constant in the $0.3<\alpha<0.7$ range, and its value was found to be $E_a=163\pm11$ kJ/mol. Within the limits of experimental errors, this value is close to 159 kJ/mol, reported by Ryšavá et al. [21]. In contrast, the activation energy for a powder sample is ca. 70% higher, being $E_a=276\pm7$ kJ/mol. Observed differences can be explained by the fact that the crystallization of a powder sample takes place at lower temperatures due to non-negligible concentra-

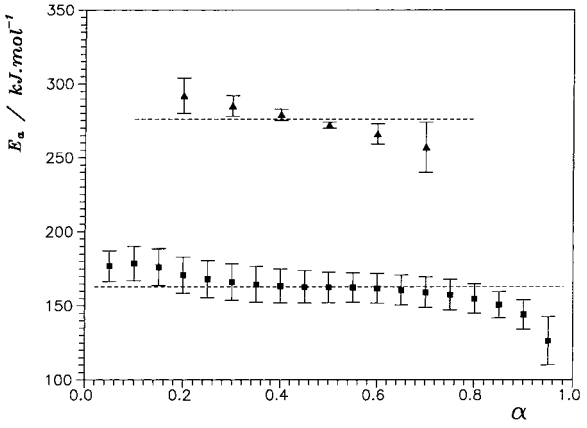

Fig. 4. The apparent activation energy as a function of fractional conversion calculated from DSC data for the crystallization of bulk (■) and fine powder sample (▲) of $(GeS_2)_{0.3}$ $(Sb_2S_3)_{0.7}$ glass (see Fig. 3). Broken lines correspond to an average value of E_a calculated in the $0.3\leq\alpha\leq0.7$ range.

tion of surface nuclei and the crystals grow at a higher viscosity of supercooled melt. Consequently, the apparent activation energy increases. A more pronounced variation of E_a versus α probably indicates a more complex mechanism of the crystallization process.

As discussed in Section 2.3, one of the most popular tests of the applicability of the JMA equation is the linearity of the double logarithmic plots vs. ln t or $1/T$. Such plots obtained from isothermal and non-isothermal DSC data for crystallization of $(GeS_2)_{0.3}$ $(Sb_2S_3)_{0.7}$ glass (see Fig. 3) are shown in Fig. 5. It seems that these plots are linear. The kinetic exponent obtained from isothermal data by using Eq. (13) was found to be $m=3.0\pm0.2$. The same value has been obtained for non-isothermal data by using Eq. (14) and $E_a=163$ kJ/mol. This result would imply that the JMA model is valid for crystallization kinetics of the bulk and powder sample. Nevertheless, the $y(\alpha)$ and $z(\alpha)$ functions shown in Figs. 6 and 7 clearly reveal that the JMA model is valid only for the non-isothermal crystallization of the bulk sample, and it is not fulfilled for isothermal crystallization of a powder sample. There are small but noticeable differences among the curves for different heating rates as well as for isothermal temperatures. These differences can probably be attributed to lower thermal contact between the bulk sample and the temperature sensor (non-isothermal data) or to errors in baseline approximation (isothermal data). Such problems are expected for this

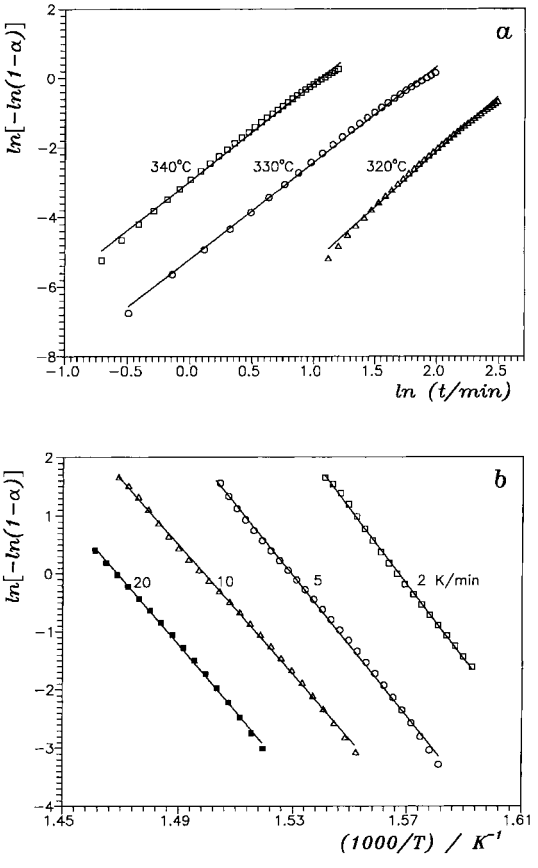

Fig. 5. The double logarithmic plots obtained from DSC data shown in Fig. 3.

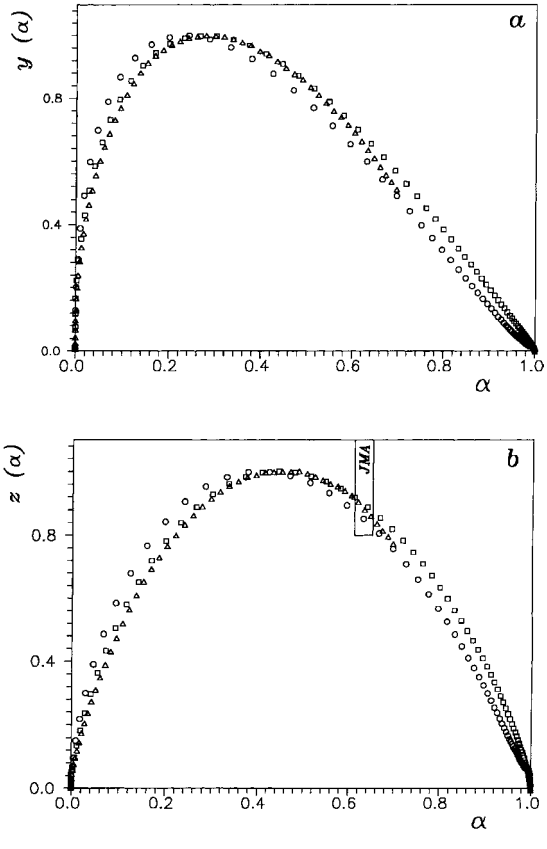

Fig. 6. Normalized $y(\alpha)$ and $z(\alpha)$ function obtained by transformation of isothermal DSC data for the crystallization of fine powder $(GeS_2)_{0.3}$ $(Sb_2S_3)_{0.7}$ glass (Fig. 3a). The temperature is shown by points: 340°C (□); 330°C (○); 320°C (△). Solid lines show the typical interval of α_P^{∞} values for the JMA model.

material as the crystallization enthalpy ΔH_c is relatively low. Nevertheless, the basic assumptions formulated in Section 2.1 seem to be fulfilled. The maximum of the $z(\alpha)$ function falls in the range predicted for the JMA model. The value of the kinetic exponent $m=3$ can be obtained from the maximum of the $y(\alpha)$ function. Somewhat lower value $m\cong 2.8$ has been calculated using the method proposed by Ozawa [18] (see Section 2.3). Any tendency for secondary crystallization has not been observed in this case. This value of the kinetic exponent corresponds to three-dimensional crystal growth of an orthorhombic Sb_2S_3 formed during the crystallization process. Such crystalline phase exhibits relatively high entropy of fusion; and, therefore, one can expect three-dimensional crystal growth [24]. These conclusions were confirmed by microscopy and X-ray diffraction analysis. Fig. 8 shows scanning electron microscope photographs of crystallized powder and bulk sample of $(GeS_2)_{0.3}$ $(Sb_2S_3)_{0.7}$ glass. The crystallites in powder sample exhibit a rod-like morphology with relatively low compactness which reveals low dimensionality of crystal growth from numerous nucleation sites. In contrast, there are relatively big three-dimensional crystals grown in the bulk sample suggesting the value of the kinetic exponent should be close to 3.

The crystallization behavior of different samples can easily be compared in the α_M–α_P^{∞} plot as shown in Fig. 9. The present results are combined with some previously published data [22,23]. The value of α_P^{∞} for a fine powder sample (<1 μm) is considerably lower than corresponds to the JMA model. There are notable differences between isothermal and non-isothermal experiments. Such behavior clearly indicates a more

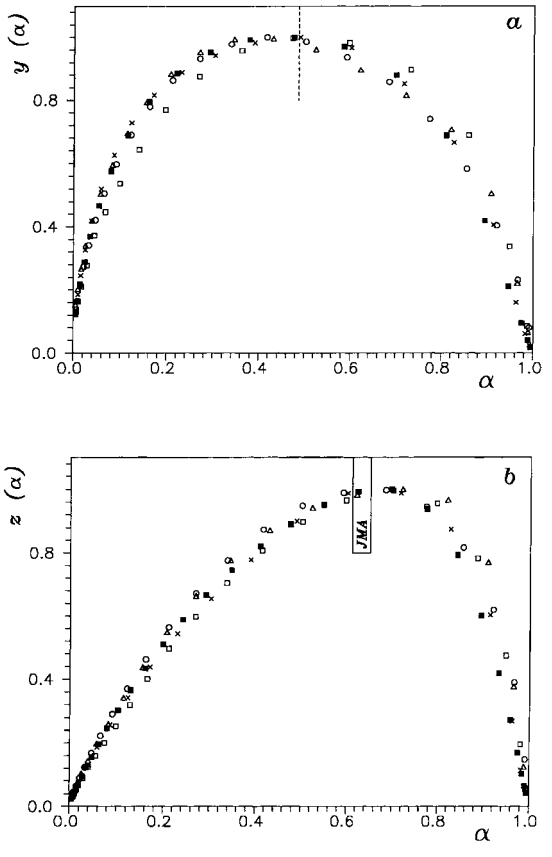

Fig. 7. Normalized $y(\alpha)$ and $z(\alpha)$ function obtained by transformation of non-isothermal DSC data for the crystallization of bulk $(GeS_2)_{0.3}$ $(Sb_2S_3)_{0.7}$ glass (Fig. 3b). The heating rates are shown by points: 2 K/min (□); 5 K/min (○); 10 K/min (△); 15 K/min (×); 20 K/min (■). The broken line corresponds to the theoretical α_M value for the JMA model (m=3). Solid lines show the typical interval of α_P^∞ values for the JMA model.

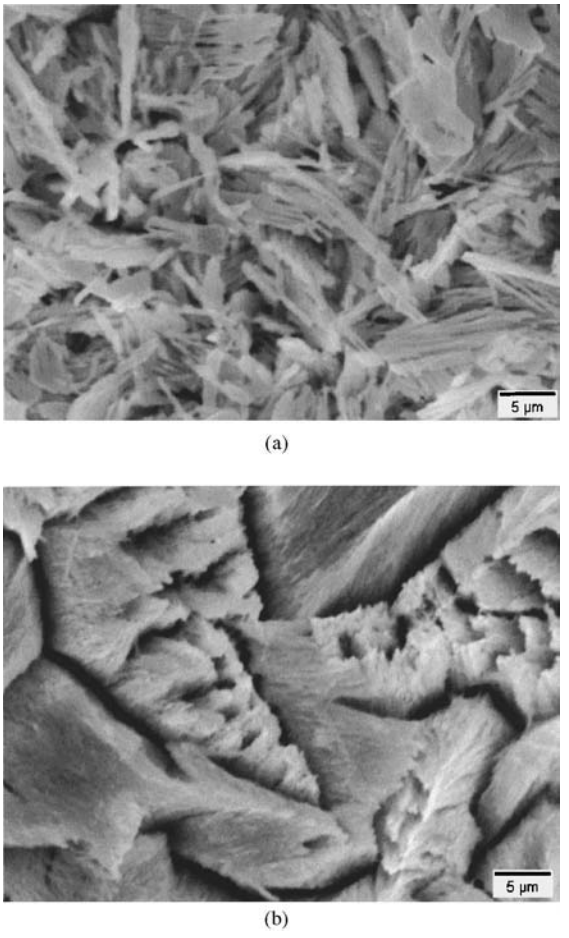

Fig. 8. Scanning electron microscope photograph showing morphology of Sb_2S_3 crystals grown in $(GeS_2)_{0.3}$ $(Sb_2S_3)_{0.7}$ glass: (a) powder sample; (b) bulk sample. A fresh fracture of crystallized sample has been etched in an aqueous solution of NaOH.

complex crystallization mechanism. The coarse powder sample (<100 μm) exhibit a slightly higher value of α_P^∞, but it is still below the value typical for the JMA model. However, the values of α_M and α_P^∞ for the bulk sample correspond well to the crystallization of three-dimensional crystals, and the kinetic exponent m is close to 3, which is consistent with the value obtained from double logarithmic plot and the maximum of the $y(\alpha)$ plot.

As mentioned above, the JMA model is valid in non-isothermal conditions provided that a new crystalline phase grows from a constant number of nuclei and all nucleation is completed before the macroscopic crystal growth started. This so-called site saturation is an important condition for the isokinetic crystallization process where the crystallization rate is defined only by temperature and does not depend on the previous thermal history [6]. In the light of these facts, it seems that the nucleation and growth processes are probably overlapped for a fine powder sample. Therefore, the overall crystallization cannot be described by the JMA model. Mutual overlapping of the nucleation and growth phases is obviously lower for a coarse powder sample but, still, the JMA model is not valid in this case. It seems that in the bulk sample the nucleation is completed before the growth phase is

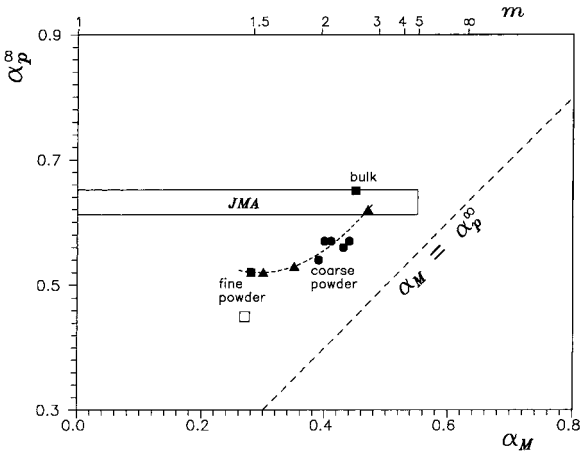

Fig. 9. The α_P^∞–α_M plot for the crystallization of $(GeS_2)_{0.3}(Sb_2S_3)_{0.7}$ glass. Full lines correspond to the limits of applicability of the JMA model. Points correspond to non-isothermal data (■) and isothermal data (□). Other data are taken from Ref. [22] (●), and Ref. [23] (▲). The dotted line is drawn as a guide to the eye. The broken line shows the theoretical limit $\alpha_M = \alpha_P^\infty$.

started and, therefore, the condition of the validity of the JMA model in non-isothermal conditions is fulfilled. A fine powder sample exhibits a lower value of α_M than corresponds to the bulk sample, which reveals a lower influence of the crystallized phase due to dominant surface nucleation. These conclusions were confirmed by direct microscopic observations.

4.2. Crystallization kinetics of zirconia gel

It is known that the metastable tetragonal polymorph crystallizes during the heating of hydrous zirconia gel [25]. Although the crystallization of *t*-ZrO_2 phase have been studied by many authors [26–32] the detailed mechanism of its formation is still not clear. Aronne et al. [30] and Ramanathan et al. [31] interpreted their experimental data within the JMA model and the calculated kinetic exponent (m=2.7 and m<1, respectively) has been attributed to the dimensionality of crystal growth. However, the experimental data have not been compared directly with the theoretical model or the $z(\alpha)$ function and, therefore, it is difficult to verify whether such an interpretation is consistent or not. Recently, it has been found that the crystallization kinetics of *t*-ZrO_2 nanocrystals in partially dried zirconia gel is strongly affected by the water content retained in dried gel [32]. The crystal-

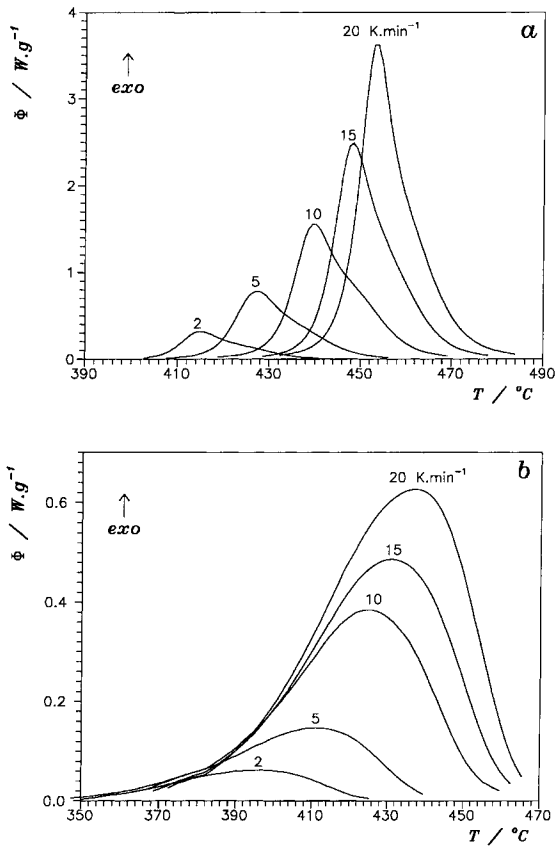

Fig. 10. Non-isothermal DSC data for the crystallization of ZrO_2 gel: (a) *as prepared* sample; (b) partially crystallized sample after a heat treatment at 370°C for 60 min (42% crystallinity).

lization process starts when practically all the water is removed (at the onset of the DSC crystallization peak the corresponding weight loss is ca. 13.4% and the final weight loss is 13.7% of the initial sample weight). Thus, in this case, the isothermal measurements cannot be used because the exothermic crystallization is partially overlapped by the endothermic effect of water evaporation.

Fig. 10 shows non-isothermal crystallization data for *as prepared* zirconia gel and a partially crystallized sample obtained after heat treatment at 370°C for 60 min. The enthalpy change $-\Delta H_c$ associated with these crystallization processes was found to be -157 ± 4 and -91 ± 4 J/g for *as prepared* and partially crystallized sample, respectively. Therefore, the crystallinity of the partially crystalline sample is ca. 42%. The activation energy E_a calculated by isoconver-

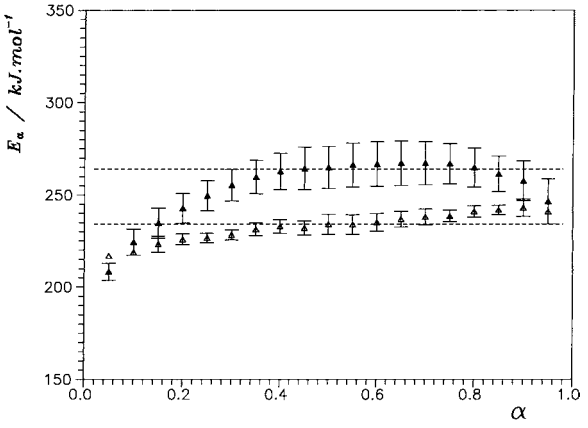

Fig. 11. The apparent activation energy as a function of fractional conversion calculated from DSC data for the crystallization of ZrO_2 gel (see Fig. 10), for *as prepared* sample (▲) and partially crystallized sample (△). Broken lines correspond to an average value of E_a calculated in the $0.3 \leq \alpha \leq 0.7$ range.

sional method using these DSC data is plotted as a function of fractional conversion in Fig. 11. The activation energy is practically constant in the $0.3<\alpha<0.7$ range, being $E_a=264\pm11$ kJ/mol for an *as prepared* sample and $E_a=234\pm4$ kJ/mol for the partially crystallized sample. The activation energy slightly decreases with increasing crystallinity of the zirconia gel [32]. The difference of 37 kJ/mol is probably associated with the nucleation process taking place in the *as prepared* sample which is no longer operative in the case of the partially crystalline sample.

Fig. 12 shows the double logarithmic plots vs. $1/T$ obtained from non-isothermal crystallization data of the *as prepared* zirconia gel and the partially crystallized sample (see Fig. 10). The plots are clearly nonlinear for the *as prepared* sample, indicating that the JMA model cannot be applied. On the other hand, the double logarithmic plots are linear for the partially crystallized sample. The kinetic exponent obtained from the slope of these plots by using Eq. (14) and $E_a=234\pm4$ kJ/mol was found to be $m=1.05\pm0.04$. A very similar value of $m\cong1.07\pm0.04$ has been obtained by using the method proposed by Ozawa [18] (see Section 2.3). Practically identical conclusions can also be obtained from the $y(\alpha)$ and $z(\alpha)$ functions. Fig. 13 shows the $y(\alpha)$ and $z(\alpha)$ plots for the crystallization of *as prepared* zirconia gel. It is evident that these

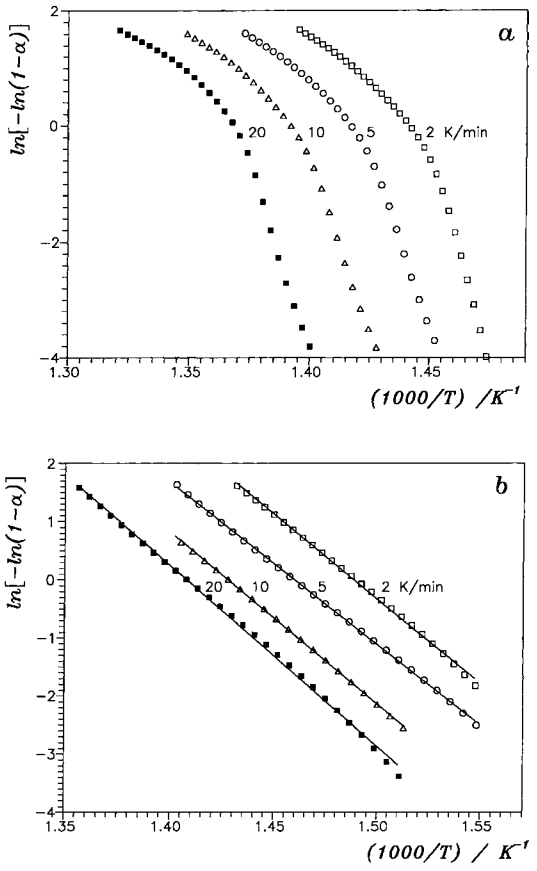

Fig. 12. The double logarithmic plots obtained from DSC data that are shown in Fig. 10.

functions are nearly invariant with respect to heating rate. The maximum of the $z(\alpha)$ function is considerably lower than the value predicted for the JMA model. However, there is a shoulder that appears close to $\alpha\cong0.632$. This rather complicated shape of the $z(\alpha)$ function can be explained assuming that the nucleation and growth processes are partially overlapped at the beginning of the DSC peak [32]. However, it seems that the nucleation process is negligible for $\alpha>0.5$ and zirconia crystals are growing from a practically constant number of nuclei. Fig. 14 shows the $y(\alpha)$ and $z(\alpha)$ plots for the crystallization of partially crystalline (42%) zirconia gel. The maximum of the $z(\alpha)$ function is located close to the value $\alpha_P^{\infty}\cong0.63$ predicted for the JMA model. The $y(\alpha)$ function decreases almost linearly; i.e. $y(\alpha)\propto(1-\alpha)$ corresponds to the kinetic exponent $m=1$.

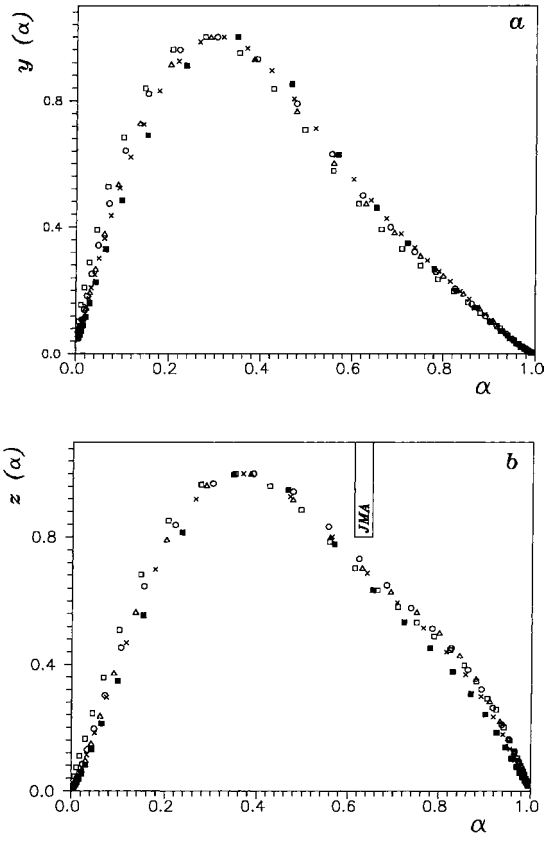

Fig. 13. Normalized $y(\alpha)$ and $z(\alpha)$ function obtained by transformation of non-isothermal DSC data for the crystallization of *as prepared* ZrO_2 gel (Fig. 10a). The heating rates are shown by points: 2 K/min (□); 5 K/min (○); 10 K/min (△); 15 K/min (×); 20 K/min (■). Solid lines show the typical interval of α_P^{∞} values for the JMA model.

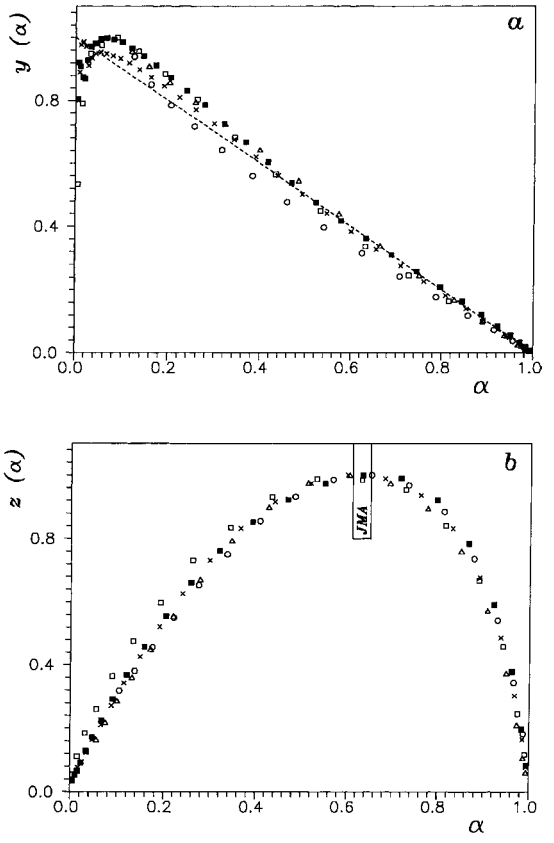

Fig. 14. Normalized $y(\alpha)$ and $z(\alpha)$ function obtained by transformation of non-isothermal DSC data for the crystallization of partially crystallized ZrO_2 gel (Fig. 10b). The heating rates are shown by points: 2 K/min (□); 5 K/min (○); 10 K/min (△); 15 K/min (×); 20 K/min (■). The broken line corresponds to the first-order kinetic model for $m=1$. Solid lines show the typical interval of α_P^{∞} values for the JMA model.

The crystallization behavior of *as prepared* and partially crystallized zirconia samples can be easily visualized in the α_M–α_P^{∞} plot, shown in Fig. 15. The samples containing lower content of crystalline phase (<25%) do not correspond to a simple crystallization kinetics as expressed by the JMA model and the value of α_P^{∞} is considerably lower than 0.6. Such behavior is a consequence of the fast increase of the initial crystallization rate. This acceleration can be due to a secondary nucleation induced by the crystal growth. An alternative explanation is associated with the adiabatic temperature drift in the amorphous gel as the crystallization heat is released. In the latter case, however, the shape of the $z(\alpha)$ function should be sensitive to heating rate, which was not observed. The crystallization rate is lower for partially crystallized samples (crystallinity >40%) and the maximum of the $z(\alpha)$ function is $\alpha_P^{\infty} \cong 0.63$ and the $y(\alpha)$ function linearly decreases. Therefore, the JMA model can be used for the description of the crystallization rate, and the value of the kinetic exponent should be close to unity as has been anticipated above. This value is also expected [33] when crystallite dimensions are sufficiently small and the rate of crystallization is controlled by nucleation in assemblage of similar particles. Therefore, one can expect that numerous and rather small crystals will be formed in the zirconia gel during the crystallization process. The experimental results support these expectations. Electron microscopy observations revealed

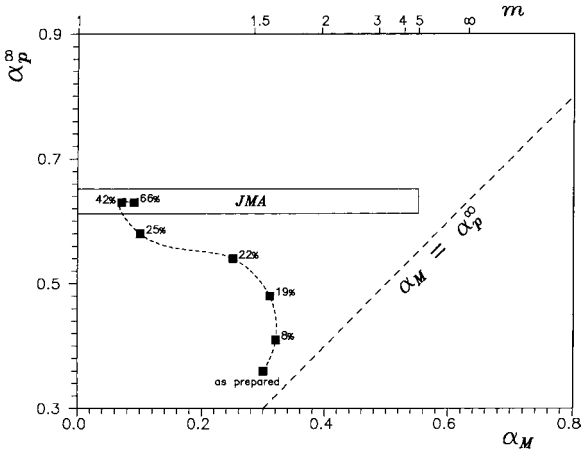

Fig. 15. The α_P^∞–α_M plot for the crystallization of the ZrO_2 gel. Full lines correspond to the limits of applicability of the JMA model. Points (■) are taken from Ref. [32] and they correspond to non-isothermal data for different crystallinity shown as a number next to the points. The dotted line is drawn as a guide to the eye. The broken line shows the theoretical limit $\alpha_M=\alpha_P^\infty$.

that *t*-ZrO_2 nanocrystals (≈13 nm in size) are formed after heat treatment of *as prepared* zirconia gel [32]. Similar average crystallite size was also estimated from corrected halfwidth of (0 1 1) X-ray diffraction peak. The nanocrystallization of the zirconia gel is consistent with the mechanism of hydrolytic polymerization of zirconyl species suggested by Clearfield [34].

4.3. Autocatalytic behavior of the crystalization kinetics

The crystallization kinetics of amorphous solids is usually interpreted in terms of the JMA model. However, strictly speaking, this model is valid in isothermal conditions and it can be rigorously applied to transformations involving nucleation and growth only in a limited number of special cases in non-isothermal conditions. Under the restrictions outlined by Henderson [5,6] an example of a system which allows the non-isothermal application of the JMA model is one in which entire nucleation process takes place during early stages of the transformation and becomes negligible afterward. In this case, the crystallization rate is defined only by temperature and does not depend on the previous thermal history. Nevertheless, even in this case the applicability of the JMA model under non-isothermal conditions should be critically examined, in particular, the meaning of the kinetic exponent *m*.

In Sections 4.1 and 4.2, we have shown that it is convenient to discuss crystallization kinetics in terms of α_M–α_P^∞ plot based on the maxima of the $y(\alpha)$ and $z(\alpha)$ function. The validity of the JMA can easily be verified checking the maximum α_P^∞ of the $z(\alpha)$ function. If the maximum falls into the $0.61 \leq \alpha_P^\infty \leq 0.65$ range then the experimental data probably correspond to the JMA model. If the maximum is shifted to lower values of fractional conversion ($\alpha_P^\infty < 0.6$) the conditions of validity of the JMA model are not fulfilled. Such a displacement indicates increasing complexity of the process and can be caused, for example, by the influence of surface nucleation. Nevertheless, the complex behavior can also be observed when the temperature distribution within the sample is affected considerably by liberation of the crystallization heat at the growth interface [6]. If the dimensions of the crystallized phase are small, the rate of the process is controlled by nucleation in assemblage of similar particles [33], and the kinetic exponent is $m=1$. The maximum of the $y(\alpha)$ function is then close to zero, i.e. $\alpha_M=0$. However, if the maximum of the $y(\alpha)$ function is shifted to higher values, it clearly indicates an increasing influence of the product (i.e. crystallized phase) to the overall crystallization kinetics. A typical example is spherulite crystal growth morphology where the spatial constrains in highly viscous media play an important role and the crystallized phase further increases the rate of the process in the direction preferred.

Such autocatalytic behavior has been observed for many crystallization processes [12,22,23,32] and can be described by means of an empirical two parameter model [9,35]:

$$f(\alpha) = \alpha^M (1-\alpha)^N \tag{17}$$

where the parameters *M* and *N* define relative contributions of acceleratory and decay regions of the kinetic process. It was shown [36] that this two parameter autocatalytic model is physically meaningful only for $M<1$. The maxima of the $y(\alpha)$ and $z(\alpha)$ depend on the value of the kinetic exponents *M* and *N*. The maximum α_M of the $y(\alpha)$ function can be expressed as

$$\alpha_M = \frac{M}{M+N} \tag{18}$$

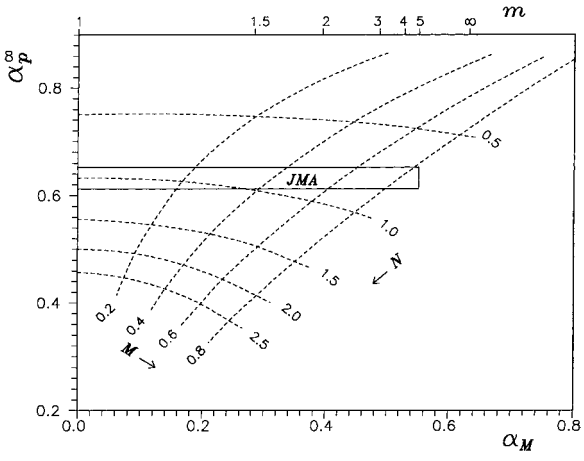

Fig. 16. The α_P^∞–α_M plot for the two parameter autocatalytic model defined by Eq. (17). The dotted lines show the influence of kinetic exponents M and N. Full lines correspond to the limits of applicability of the JMA model.

Nevertheless, the maximum α_P^∞ of the $z(\alpha)$ function cannot be expressed in an analytical form and has to be obtained by the numerical solution of Eq. (A.9). Fig. 16 shows α_M–α_P^∞ diagram calculated using Eqs. (A.3) and (A.9) for a constant value of the parameters M and N of the autocatalytic model. It is evident that the JMA model is a special case of the two-parameter model as already pointed out by Šesták [9]. Therefore, the model defined by Eq. (17) is a plausible mathematical description for the nucleation and growth processes in non-crystalline solids. The data shown in Figs. 9 and 15 can be also described by this model [23,32]. It was shown that TTT diagrams predicted for this model correspond well to experimental data [37]. The increasing value of the kinetic exponent M indicates a more important role of the crystallized phase on the overall kinetics. It seems that a higher value of the kinetic exponent $N>1$ means increasing complexity. However, the temptation to equate parameters M and N with a definite crystallization mechanism should be avoided, and too much physical significance should not be attached to the numerical values of what is essentially a phenomenological convenience. In particular, this warning applies to processes exhibiting a complex behavior. Therefore, it seems that meaningful conclusions concerning the real mechanism of the process should always be based on other types of complementary evidence, including microscopic observations together with all other relevant information.

5. Conclusions

The presented results clearly indicate that the Johnson–Mehl–Avrami (JMA) model has limited validity both in isothermal and non-isothermal conditions, and it is strongly recommended to always test its applicability for a particular crystallization process. In addition to this validity test, there are several basic assumptions implicitly involved in kinetic treatment of isothermal and non-isothermal TA data which should also be checked before any kinetic analysis is made.

A unified approach based on two functions $y(\alpha)$ and $z(\alpha)$ obtained by a simple transformation of experimental data is proposed, allowing a testing of the validity of the JMA model as well as the basic assumptions in kinetic analysis. The $y(\alpha)$ and $z(\alpha)$ functions exhibit maxima at α_M and α_P^∞, respectively ($\alpha_M<\alpha_P^\infty$). Their position and shape should be invariant with respect to procedural variables such as heating rate (non-isothermal conditions) and temperature (isothermal conditions). The shape of these plots should also be identical for isothermal and non-isothermal data. The validity of the JMA model can easily be verified by checking the maximum α_P^∞ of the $z(\alpha)$ function. If the maximum falls into $0.61 \leq \alpha_P^\infty \leq 0.65$ range then experimental data probably correspond to the JMA model.

It is convenient to describe crystallization kinetics in terms of α_M–α_P^∞ plot. This diagram helps to visualize the complexity of the crystallization process as well as to verify the applicability of the JMA model. The two parameter autocatalytic model includes the JMA model as a special case and, therefore, is a plausible mathematical description for the nucleation and growth processes in amorphous solids. The main advantage of the two parameter model is its potential to describe quantitatively even complex crystallization processes.

Acknowledgements

This work was supported by the grant Agency of the Czech Republic under grants No. 203/96/0184, 104/97/0589 and 202/98/K002.

Appendix A. Transformation of DSC data

A.1. The $y(\alpha)$ function

In isothermal conditions the $y(\alpha)$ function can be expressed from Eq. (6) as

$$y(\alpha) = \phi = B_i f(\alpha) \tag{A.1}$$

where $B_i = \Delta H_c A \exp(-E_a/RT)$ is a constant. Thus, by differentiation of Eq. (A.1) with respect to α, we obtain

$$y'(\alpha) = B_i f'(\alpha) \tag{A.2}$$

By setting Eq. (A.2) equal to zero, we obtain the condition which must be fulfilled by α_M at the maximum of the $y(\alpha)$ function

$$f'(\alpha_M) = 0 \tag{A.3}$$

Therefore, the shape of the $y(\alpha)$ function is formally identical with the kinetic model function $f(\alpha)$, and the value of α_M can be obtained from Eq. (A.3).

In non-isothermal conditions, the exponential term $\exp(-E_a/RT)$ in Eq. (A.1) is not constant and, therefore, the $y(\alpha)$ function is defined as [12]:

$$y(\alpha) = \phi \exp\left(\frac{-E_a}{RT}\right) = B_n f(\alpha) \tag{A.4}$$

where $B_n = \Delta H_c A$ is a constant. The $y(\alpha)$ is usually normalized within the (0 1) range and, therefore, its shape should be identical both in isothermal and non-isothermal conditions.

A.2. The $z(\alpha)$ function

By integration of Eq. (4) in isothermal conditions, the following equation is obtained

$$g(\alpha) = \int_0^\alpha \frac{d\alpha}{f(\alpha)} = A \exp\left(\frac{-E_a}{RT}\right) t \tag{A.5}$$

By inserting this equation into Eq. (2), one can obtain the expression

$$\left(\frac{d\alpha}{dt}\right) = \frac{1}{t}(\alpha) g(\alpha) \tag{A.6}$$

Combining Eqs. (A.6) and (3), we obtain the following expression for the $z(\alpha)$ function in isothermal conditions

$$z(\alpha) = \phi t = C_i f(\alpha) g(\alpha) \tag{A.7}$$

where $C_i = \Delta H_c$ is a constant. Differentiating Eq. (A.7) with respect to α, we obtain

$$z'(\alpha) = C_i [f'(\alpha) g(\alpha) + 1] \tag{A.8}$$

By setting Eq. (A.8) equal to zero, we obtain the condition that must be fulfilled by α_P^∞ at the maximum of the $z(\alpha)$ function [13]:

$$-f'(\alpha_P^\infty) g(\alpha_P^\infty) = 1 \tag{A.9}$$

The $g(\alpha)$ function can be written for the JMA model as

$$g(\alpha) = [-\ln(1-\alpha)]^{1/m} \tag{A.10}$$

Comparing Eqs. (A.9) and (A.3), it follows that $\alpha_P^\infty = \alpha_M$ holds only for an infinite $g(\alpha)$. This condition can be considered as a theoretical limit of any kinetic model; and, for the JMA model, it is fulfilled for an infinite value of the kinetic exponent m. Therefore, the maximum of the $z(\alpha)$ function is always located at higher values of α than the maximum of the $y(\alpha)$ function.

If the temperature rises at a constant rate $\beta = dT/dt$, then, after the integration of Eq. (4), one can obtain the following equation

$$g(\alpha) = \frac{AT}{\beta} \exp\left(\frac{-E_a}{RT}\right) \pi\left(\frac{-E_a}{RT}\right) \tag{A.11}$$

where $\pi(E_a/RT)$ is an approximation of the temperature integral which has to be introduced because the $K(T)$ term cannot be integrated analytically [9]. Combining Eqs. (A.11) and (6), we can obtain the following expression for the $z(\alpha)$ function in non-isothermal conditions

$$z(\alpha) = \phi T \pi\left(\frac{E_a}{RT}\right) = \Delta H_c \, \beta f(\alpha) g(\alpha) \tag{A.12}$$

It was shown [14] that in the case of the $z(\alpha)$ function the approximation $\pi \cong RT/E_a$ is sufficiently accurate. Then the $z(\alpha)$ function can be expressed as

$$z(\alpha) = \phi T^2 = C_n f(\alpha) g(\alpha) \tag{A.13}$$

where $C_n = \Delta H_c \, \beta E_a/R$ is a constant and, therefore, the value of the α_P^∞ characteristic for any kinetic model can be obtained from Eq. (A.9).

The $z(\alpha)$ function is usually normalized within the (0, 1) range and its shape, as well as the condition for the maximum, should be identical both in isothermal and non-isothermal conditions.

A.3. The generalized $y(\alpha)$ and $z(\alpha)$ functions

A very useful concept of generalized time introduced by Ozawa [8,15] can be used to obtain the generalized $y(\alpha)$ and $z(\alpha)$ functions. For Arrhenius type rate constant the generalized time, θ, is defined as

$$\theta = \int_0^t \exp\left(\frac{-E_a}{RT}\right) dt \tag{A.14}$$

Differentiating Eq. (A.14) with respect to time we obtain

$$\left(\frac{d\theta}{dt}\right) = \exp\left(\frac{-E_a}{Rt}\right) \tag{A.15}$$

Combining Eqs. (4), (5) and (A.15) we obtain the following general expression for the $y(\alpha)$ function:

$$y(\alpha) = \left(\frac{d\alpha}{d\theta}\right) = Af(\alpha) \tag{A.16}$$

The function $(d\alpha/d\theta)$ has already been used for the description of thermal decomposition processes [38,39].

By integrating of Eq. (4) the following equation is obtained:

$$g(\alpha) = \int_0^\alpha \frac{d\alpha}{f(\alpha)} = A\theta \tag{A.17}$$

By combining Eqs. (A.17) and (A.16), we obtain the following general expression for the $z(\alpha)$ function:

$$z(\alpha) = \left(\frac{d\alpha}{d\theta}\right)\theta = f(\alpha)g(\alpha) \tag{A.18}$$

Eqs. (A.16) and (A.18) are the generalized expression for the $y(\alpha)$ and $z(\alpha)$ function. These functions depend on two fundamental variables only; i.e. the fraction crystallized and the generalized time, and they can easily be applied for the analysis of both isothermal and non-isothermal processes.

References

[1] M. Avrami, J. Chem. Phys. 7 (1939) 1103.
[2] M. Avrami, J. Chem. Phys. 8 (1940) 212.
[3] M. Avrami, J. Chem. Phys. 9 (1941) 177.
[4] J.W. Christian, The Theory of Transformations in Metals and Alloys, 2nd Edition, Pergamon Press, New York, 1975, 525 pp.
[5] D.W. Henderson, J. Therm. Anal. 15 (1979) 325.
[6] D.W. Henderson, J. Non-Cryst. Solids 30 (1979) 301.
[7] M.P. Shepilov, D.S. Baik, J. Non-Cryst. Solids 171 (1994) 141.
[8] T. Ozawa, Bull. Chem. Soc. Jpn. 57 (1984) 639.
[9] J. Šesták, Thermophysical Properties of Solids. Their Measurements and Theoretical Analysis, Elsevier, Amsterdam, 1984, Chapters 8 and 9, pp. 172–254.
[10] R. Serra, J. Sempere, R. Nomen, Thermochim. Acta 316 (1998) 37.
[11] R. Serra, J. Sempere, R. Nomen, J. Therm. Anal. 52 (1998) 933.
[12] J. Málek, Thermochim. Acta 138 (1989) 337.
[13] J. Málek, Thermochim. Acta 200 (1992) 257.
[14] J. Málek, Thermochim. Acta 267 (1995) 61.
[15] T. Ozawa, Thermochim. Acta 100 (1986) 109.
[16] H.L. Friedman, J. Polym. Sci., Part C. Polym. Lett. 6 (1964) 183.
[17] T. Ozawa, J. Therm. Anal. 31 (1986) 547.
[18] T. Ozawa, Polymer 12 (1971) 150.
[19] N. Ryšavá, L. Tichý, Č. Barta, A. Tříska, H. Tichá, Phys. Stat. Sol. (a) 87 (1985) K13.
[20] N. Ryšavá, T. Spasov, L. Tichý, J. Therm. Anal. 32 (1987) 1015.
[21] N. Ryšavá, Č. Barta, L. Tichý, J. Mat. Sci. Lett. 8 (1989) 91.
[22] J. Málek, V. Smrčka, Thermochim. Acta 186 (1991) 153.
[23] J. Málek, E. Černošková, R. Švejka, J. Šesták, G. Van der Plaats, Thermochim. Acta 280-281 (1996) 353.
[24] K.A. Jackson, D.R. Uhlmann, J.D. Hunt, J. Crystal Growth 1 (1967) 1.
[25] J. Málek, L. Beneš, T. Mitsuhashi, Powder Diffraction 12 (1997) 96.
[26] G. Gimblett, A.A. Rahman, K.S.W. Sing, J. Chem. Tech. Biotechnol. 30 (1980) 51.
[27] P. Colomban, E. Bruneton, J. Non-Cryst. Solids 147-148 (1992) 201.
[28] T. Mitsuhashi, M. Ichihara, U. Tatsuke, J. Am. Ceram. Soc. 57 (1974) 97.
[29] J. Livage, K. Doi, C. Maziéres, J. Am. Ceram. Soc. 51 (1968) 349.
[30] A. Arone, P. Pernice, A. Marotta, J. Mat. Sci. Lett. 10 (1991) 1136.
[31] S. Ramanathan, N.C. Sini, R. Prasad, J. Mat. Sci. Lett. 12 (1993) 122.
[32] J. Málek, T. Mitsuhashi, J. Ramírez-Castellanos, Y. Matsui, J. Mater. Res. 14 (1999) 1834.
[33] M.E. Brown, D. Dollimore, A.K. Galwey, Reactions in Solid State, Elsevier, Amsterdam, 1982, Chapter 3, pp. 41–113.
[34] A. Clearfield, J. Mater. Res. 5 (1990) 161.
[35] J. Šesták, G. Berggren, Thermochim. Acta 3 (1971) 1.
[36] J. Málek, J.M. Criado, J. Šesták, J. Militký, Thermochim. Acta 153 (1989) 429.
[37] J. Málek, Sci. Pap. Univ. Pardubice, Ser. A 2 (1996) 177.
[38] N. Koga, H. Tanaka, J. Phys. Chem. 98 (1994) 10521.
[39] N. Koga, S. Takemoto, T. Nakamura, H. Tanaka, Thermochim. Acta 282-283 (1996) 81.